ACCOUNTS
of chemical research

Principles, Efficiency, and Blueprint Character of Solar-Energy Conversion in Photosynthetic Water Oxidation

HOLGER DAU* AND IVELINA ZAHARIEVA
Freie Universität Berlin, FB Physik, Arnimallee 14, D-14195 Berlin, Germany

RECEIVED ON AUGUST 11, 2009

CONSPECTUS

Photosynthesis in plants and cyanobacteria involves two protein−cofactor complexes which are denoted as photosystems (PS), PSII and PSI. These solar-energy converters have powered life on earth for approximately 3 billion years. They facilitate light-driven carbohydrate formation from H_2O and CO_2, by oxidizing the former and reducing the latter.

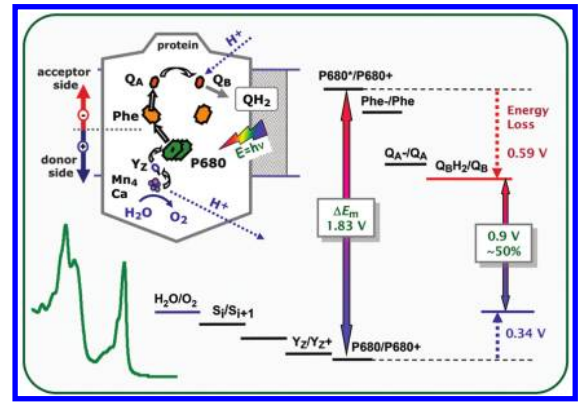

PSII splits water in a process driven by light. Because all attractive technologies for fuel production driven by solar energy involve water oxidation, recent interest in this process carried out by PSII has increased. In this Account, we describe and apply a rationale for estimating the solar-energy conversion efficiency (η_{SOLAR}) of PSII: the fraction of the incident solar energy absorbed by the antenna pigments and eventually stored in form of chemical products. For PSII at high concentrations, approximately 34% of the incident solar energy is used for creation of the photochemistry-driving excited state, P680*, with an excited-state energy of 1.83 eV. Subsequent electron transfer results in the reduction of a bound quinone (Q_A) and oxidation of the Tyr_Z within 1 μs. This radical-pair state is stable against recombination losses for approximately 1 ms. At this level, the maximal η_{SOLAR} is 23%. After the essentially irreversible steps of quinone reduction and water oxidation (the final steps catalyzed by the PSII complex), a maximum of 50% of the excited-state energy is stored in chemical form; η_{SOLAR} can be as high as 16%. Extending our considerations to a photosynthetic organism optimized to use PSII and PSI to drive H_2 production, the theoretical maximum of the solar-energy conversion efficiency would be as high as 10.5%, if all electrons and protons derived from water oxidation were used for H_2 formation. The above performance figures are impressive, but they represent theoretical maxima and do not account for processes in an intact organism that lower these yields, such as light saturation, photoinhibitory, protective, and repair processes.

The overpotential for catalysis of water oxidation at the Mn_4Ca complex of PSII may be as low as 0.3 V. To address the specific energetics of water oxidation at the Mn complex of PSII, we propose a new conceptual framework that will facilitate quantitative considerations on the basis of oxidation potentials and p*K* values.

In conclusion, photosynthetic water oxidation works at high efficiency and thus can serve as both an inspiring model and a benchmark in the development of future technologies for production of solar fuels.

Introduction

In oxygenic photosynthesis, solar energy is used to extract the two elementary particles from water which play a crucial role in chemistry and biology: electrons and protons.[1−3] This process of water-splitting is called photosynthetic water oxidation or oxygen evolution, with the latter referring to the O_2 molecules formed as a byproduct. It is facilitated by photosystem II (PSII), a cofactor−protein complex (Figure 1). Employing a second photoreaction in photosystem I (PSI), the electrons are transferred to electron acceptors of sufficiently reducing power for the reduction of atmospheric CO_2 and carbohydrate formation,

Published on the Web 11/12/2009 www.pubs.acs.org/acr
10.1021/ar900225y CCC: $71.50

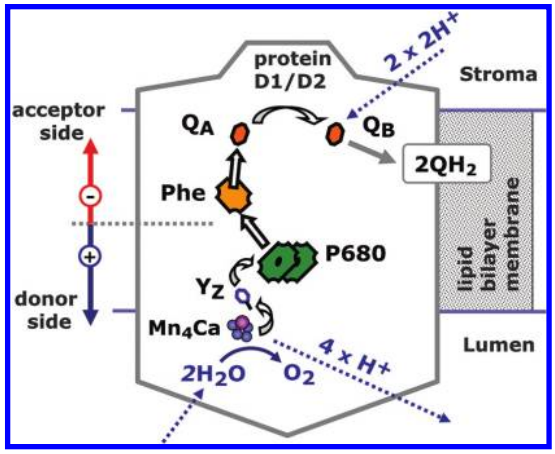

FIGURE 1. Arrangement of redox factors in PSII. The D1/D2 protein subunits harbor all essential redox factors. The proteins of the PSII core complex carrying antenna pigments (CP34, CP47) and peripheral light-harvesting complexes are not shown. The aqueous phases at the acceptor side (stroma) and donor side (lumen) are separated by a lipid bilayer (thylakoid membrane). Formation of the excited state of P680 is followed by electron transfer steps, which at the donor side resembles movement of a positively charged "hole".

essentially by incorporating the electrons and protons previously extracted from water. This process serves a dual role in biology: (i) biomass formation starting from water and carbon dioxide; (ii) utilization of solar energy to drive the synthesis of energy-rich compounds, that is, fuel production.

The latter point is of high interest in the worldwide goal for developing technologies for fuel production directly powered by solar energy. All attractive scenarios for such technologies involve light-driven water oxidation followed by use of protons and "energized electrons" for formation of molecular hydrogen (H_2) or other fuels (methane, methanol, carbohydrates, etc.). Analyzing and evaluating the function and efficiency of PSII as a water-oxidizing solar energy converter is of interest because (i) PSII needs to do its task in a photosynthetic microorganism genetically optimized for fuel (typically H_2) production and (ii) PSII serves as an inspiration and benchmark for the design of artificial systems for light-driven water oxidation.[4−6]

From the viewpoint of life on earth, PSII has been an amazing success. Presently, no synthetic system can do what PSII does when it comes to light-driven water oxidation. However, newspaper articles comparing a PSII efficiency exceeding 90% to values of 30% for the best photovoltaics cells are, to say the least, misleading. Here, we describe basic principles of PSII function and provide estimates on its energetics and solar-energy conversion efficiency.

Solar-Energy Conversion Efficiency: Rationale

First, terms are introduced that facilitate quantitative considerations. The overall efficiency of solar energy conversion, η_{SOLAR}, denotes the ratio between the incident solar energy (flux) and the fraction of this energy (flux) stored in the form of a chemical product. For PSII and other photosynthetic systems, η_{SOLAR} can be calculated as the product of three factors: (I) The *light-harvesting yield* (LHY) provides the percentage of the incident solar energy absorbed by a PSII suspension (or suspension of PSII-containing microorganisms) and used for formation of the specific excited state that drives photochemistry, that is, P680* in PSII. (II) The *fractional energy yield* (FEY) is the fraction of the excited state energy of P680* which is stored in the form of a distinct chemical product, for example, a specific radical pair. (III) The *quantum yield* (QY) describes the *probability* that after absorption and P680* formation a specific chemical product is formed. Both FEY and QY depend on the product state (Pr_i) formed.

The value of η_{SOLAR} is given by

$$\eta_{SOLAR}(Pr_i) = LHY \times FEY(Pr_i) \times QY(Pr_i) \qquad (1)$$

In the following, we will discuss, estimate, and evaluate the performance parameters of solar energy conversion by PSII, namely, LHY, FEY, QY, and η_{SOLAR}.

Light-Harvesting Yield (LHY)

As is generally the case in plant and bacterial photosynthesis, in PSII, dozens or even hundreds of protein-bound pigments absorb light energy and transfer the thereby created excited singlet-state to a single reaction-center complex where the primary photochemistry as well as secondary and tertiary redox reactions take place.[1−3] The large number of sensitizer pigments results in an effective optical absorption cross section for induction of the primary photochemistry which is roughly a hundred times higher than that for an individual pigment molecule. Therefore, the sensitizer molecules are frequently denoted as "light-harvesting" or "antenna" pigments.

The complete Photosystem II consists of a largely species-independent core, the PSII core complex, and species-dependent peripheral antenna complexes.[1−3] In the PSII core complex, light is absorbed by about 35 chlorophyll-*a* molecules (Chl *a*) and 12 carotenoids bound to the CP43, CP47, D1, and D2 subunits of the PSII core complex.[7,8] The complex of D1/D2 and cyt b559 hosts all relevant redox factors and thus may be considered as the photochemical reaction-center complex (Figure 1).

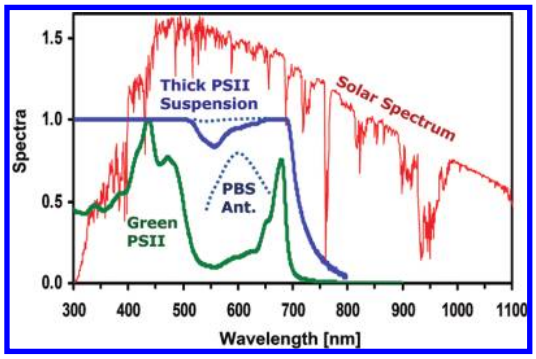

FIGURE 2. Solar spectrum and absorption spectra of plant PSII. Red line, solar spectrum in W m^{-1} nm^{-1} (spectral irradiance; for details, see text); green line, absorption spectrum of PSII particles prepared from spinach (arbitrary units); blue line, (calculated) fraction of incoming photons absorbed by an optically thick PSII suspension as encountered, for example, in a leaf or an alga culture (relative units). The broken lines indicates absorption by the phycobilisome system (PBS) of, for example, cyanobacteria.

The peripheral antenna determine the color of the organism (green, red, brown, gold, and blue algae where the latter today are classified as cyanobacteria).[1−3] The two prototypes of the peripheral antenna system are (i) the phycobilisomes membrane extrinsically attached to PSII at its stroma side and (ii) the system of a dozen or more membane intrinsic light-harvesting complex (LHC) proteins binding chlorophylls and carotenoids. The phycobilisome system is found in cyanobacteria (inter alia), whereas the membrane-intrinsic LHC system is found in green alga and all terrestrial plants.

The absorption of PSII membrane particles prepared from plants is clearly above zero for wavelengths up to about 700 nm (Figure 2). The absorption at wavelengths exceeding 680 nm and the contribution of the corresponding long-wavelength photons to induction of PSII photochemistry is well documented, but it may depend on species and growth conditions.[9−11] The phycobilisome system covers the absorption gap of Chl *a* in the green, but it does not extend the wavelength range of 300−700 nm. (Only in a rare group of cyanobacteria, Chl *d* serves as an antenna pigment and extents the absorption up to 775 nm.[12,13]) For calculation of the LHY (of a suspension, device, etc.), PSII is assumed to be present at high concentration so that most photons in the range from 300 to 700 nm are "harvested". Such high concentrations are encountered in concentrated alga suspensions of bioreactors and in some natural habitats (microbial mats, dark-green leaves, etc.).

Absorption of visible light results in the formation of excited singlet states of Chl followed by rapid excitation energy transfer and equilibration among the antenna Chl's of PSII (rapid exciton equilibration).[9,14,15] The following are observed: (i) population of the different spectral forms of chlorophyll according to a Boltzmann equilibrium, (ii) excitation of P680, a chlorophyll, or group of pigments located in the D1/D2 reaction-center complex (with maximal absorption at ∼680 nm), and (iii) induction of electron transfer from P680 to a nearby pheophytin (Phe).

The excited-state energy of P680 (E_{680}) is estimated to be 1.825 eV, the energy of a 680 nm photon. For any photon absorbed by PSII, the energy for driving the photochemistry is equal to E_{680}. The energy difference, $E_p(\lambda) - E_{680}$, is mostly thermally dissipated, reducing the energy conversion efficiency of PSII for blue-light excitation significantly.

We calculated the light-harvesting yield (LHY), that is, the fraction of the incident solar spectrum that is converted into the excited state energy of P680*, according to

$$\mathrm{LHY} = \frac{\int I_S(\lambda)\ \mathrm{LHE}(\lambda)\ \Phi_{tr}(\lambda)\ [E_{680}/E_P(\lambda)]\ \mathrm{d}\lambda}{\int I_S(\lambda)\ \mathrm{d}\lambda} \qquad (2)$$

with (i) $I_S(\lambda)$ being the (standard) spectrum of the solar radiation at ground level (here: AM 1.5, ASTM G173-03 tables, global tilt; from http://rredc.nrel.gov/solar/spectra/am1.5/; red line in Figure 2); (ii) LHE(λ) (light-harvesting efficiency) being the total absorption probability for a photon entering a "device" containing photosystems; (iii) $\Phi_{tr}(\lambda)$ being the probability for excitation energy transfer to P680; and (iv) $E_P(\lambda)$ being the photon energy.

For high concentrations of PSII, LHE(λ) can be close to 100% for λ ranging from 300 to 700 nm; also the transfer probability may be close to unity. Thus, for calculation of LHY, we used the following approximation: The product of LHE(λ) and $\Phi_{tr}(\lambda)$ equals 0.9 (90%) for λ within the 300−700 nm range; the same product equals zero for λ outside this range.

Eventually, an estimate is obtained, which likely represents an upper limit:

$$\mathrm{LHY} \approx 34\% \qquad (3)$$

Fractional Energy Yield (FEY) of Redox Products in PSII

The photon absorption by PSII pigments and P680* formation is followed by a sequence of electron transfer (ET) reactions which each result in the formation of specific radical pairs by oxidation of one redox factor at the PSII donor side or reduction of one at the acceptor side. In the scheme of Figure 3, the corresponding free-energy energy ladder is shown.[16−18] The indicated FEY values are calculated according to

$$\mathrm{FEY} = \frac{(E_{680} - |\Delta G|)}{E_{680}} \qquad (4)$$

where ΔG is the difference in free energy between the excited state of P680 and the specific radical-pair state. (We note that ΔG may be better denoted as ΔG_0; for simplicity, the subscript is dropped. Here and in the following, entropic contributions to ΔG are largely neglected so that ΔG refers to the enthalpic contribution only and thus can be considered as being approximately temperature-independent.)

Individual steps are described in the following.

(1) The ET from P680* to a specific pheophytin (Phe) is ultrafast (~3 ps) and activation-energy free.[19] The drop in free energy associated with this step is ~160 meV; less than 10% of E_{680} is lost. Notably, the mean excited state lifetime is clearly longer than a few picoseconds (~200 ps in plant PSII) mostly because the intrinsic rate of charge separation is scaled down by the probability that the excited state resides on P680.[9,14,15]

(2) Formation of the primary radical pair ($P680^+Phe^-$) is followed by fast, activationless ET to Q_A (~300 ps), a plastoquinone firmly bound to the D2 protein. The drop in free energy associated with the Phe → Q_A electron transfer is especially high so that at the level of the $Q_A^-P680^+$ radical pair almost 30% of E_{680} has been dissipated.

(3) $Q_A^-P680^+$ formation is followed by ET from a redox-active tyrosine ($Tyr_{160/161}$ of the D1 protein; denoted as Z, Tyr_Z, or Y_Z) to $P680^+$, likely coupled to a shift of the phenol proton to D1-His_{190} (proton-coupled electron transfer).

(4) Formation of the initial $Z^+Q_A^-{}_{(1)}$ state is followed by short- and long-range proton movements, which are only inadequately described as mere (dissipative) charge solvation. Prior to the oxygen-evolution step, a proton is removed within about 200 μs from the Mn complex and released into the aqueous phase, a process likely driven by the positive charge at Z^+ and conversely coupled to decrease in the free energy of the $Z^+Q_A^-$ state by about 100 meV ($Z^+Q_A^-{}_{(2)}$ at 65% of E_{680}).[20,21] Similar protonation dynamics likely are linked to most (or all) steps of the redox chemistry at the donor side (water splitting) and acceptor side (Q_B reduction and protonation).

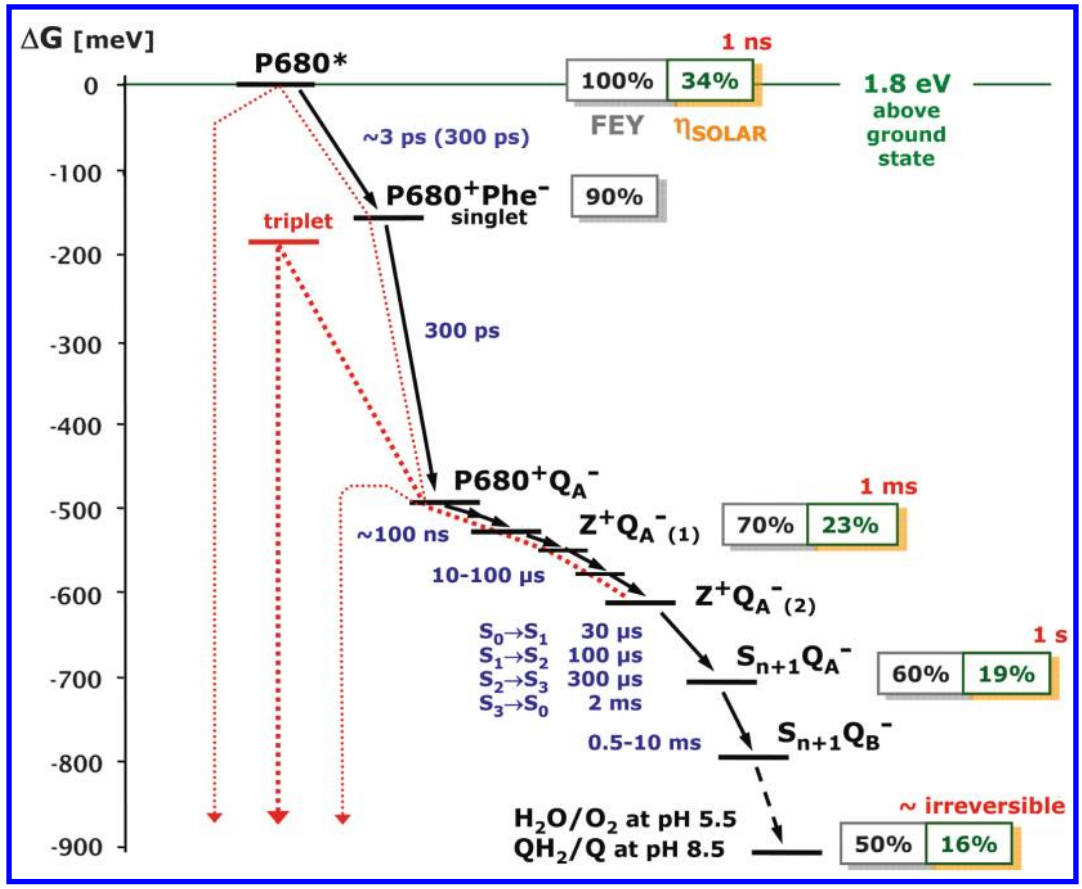

FIGURE 3. Estimated energy levels and energetic efficiencies. The fractional energy yield is given in gray boxes; η_{SOLAR} in orange boxes. Forward reactions, black arrows; loss paths, red-brown dotted lines. The numbers in red-brown (close to η_{SOLAR} boxes) indicate how long the respective state would be populated if its lifetime were determined exclusively by loss processes (order-of-magnitude estimates). The excited state of P680* lies 1.83 eV above the ground state and is chosen as the zero point of the ΔG-axis. The ΔG-axis indicates, for all states formed after P680* formation, the respective drop in free energy (in meV).

(5) The tyrosine radical oxidizes the nearby Mn_4Ca complex at a rate which depends on the number of oxidizing equivalents previously accumulated by the Mn complex. Thereby, the Mn complex undergoes the $S_i \rightarrow S_{i+1}$ transition.[20] (S_i denotes a state of the Mn complex with i accumulated oxidizing equivalents.) The Mn complex eventually catalyzes water oxidation and O_2 formation.[18,22] Driven by four photons, it reaches the S_4 state and only then O_2 is released, coupled to reversal toward the S_0 state.

(6) At the acceptor side, an electron is transferred from Q_A to the secondary quinone acceptor, Q_B. A second photon initiates a second $Q_A \rightarrow Q_B$ ET, resulting in doubly reduced Q_B which leaves the PSII complex in the form of QH_2, a mobile electron (and proton) carrier.

(7) The reduction equivalents carried by QH_2 represent the "high-energy product" of the light-driven reactions in PSII. They can drive reductive processes at a redox potential that is by up to 0.9 V more positive than the midpoint potential of water oxidation. The latter figure requires an explanation. When photosynthetic organisms are exposed to light, the lumen space (donor side) is acidified whereas the stroma pH (acceptor side) increases. Assuming that the working pH is 5.5 at the donor side and 8.5 at the acceptor side, the midpoint potentials of QH_2/Q and H_2O/O_2 are about +0.0 and +0.9 V (versus NHE), respectively, resulting in a potential difference of 0.9 V. Thus, independent of all details of the preceding charge transfer reactions, the energy stored by transfer of one electron from water to the mobile organic acceptor maximally is 0.9 eV, that is around 50% of E_{680}.

We note that, in intact photosynthetic organisms, both the light-induced membrane potential and the pH gradient across the thylakoid membrane (jointly constituting the proton motive force, PMF) are exploited to drive the formation of ATP from ADP, increasing the figure of 50% to a level possibly as high as 60%.[1−3] This "side reaction" is difficult to quantify and here not considered in more detail.

(8) The above considerations are on solar energy conversion by PSII. Having in mind the biotechnological approach of using genetically optimized photosynthetic organisms for hydrogen production, we extend the above considerations to include the complete set of photosynthetic light reactions. In oxygenic photosynthesis, the reduced plastoquinone molecules (QH_2) feed electrons in an electron transfer chain, thereby (i) increasing the PMF by intricate coupling of redox chemistry with proton transport and (ii) providing reducing equivalents to a second photosystem denoted (for historical reasons) as PSI. The PSI threshold energy corresponds to 700 nm (P700 instead of P680, $E_{700} = 1.77$ eV). Its design is similar with respect to the fast energy transfer and ET processes which are mediated by pigments and redox factors in the low-dielectric, membrane-intrinsic regions of the cofactor−protein complex but necessarily different for the slower redox reactions at the donor and acceptor side.[1−3] The reducing equivalents provided by PSI normally are used for CO_2 reduction and eventually carbohydrate formation, but also they can be used for driving proton reduction and H_2 formation by enzymes denoted as hydrogenases (Figure 4). Irrespective of mechanistic details, we can estimate the maximal fractional energy yield of the overall process from the threshold energies and the redox potential differences of H_2/H^+ (E_{mH_2}) and H_2O/O_2 (E_{mO_2}). At unphysiological (but technologically relevant) partial pressures of 1 bar for H_2 and O_2, the following equation holds for the fractional energy yield (FEY) of the overall reaction of H_2 production from water:

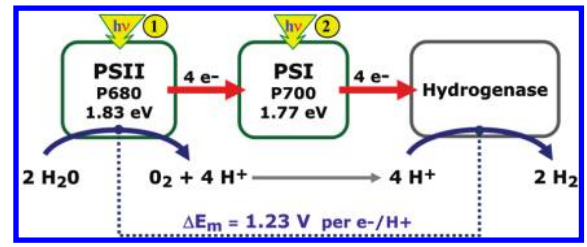

FIGURE 4. Scheme on light-driven H_2 formation by PSII and PSI. The corresponding maximal η_{SOLAR} is estimated to be 10.5%.

$$\mathrm{FEY}(H_2) = (eE_{mO_2} - eE_{mH_2})/(E_{680} + E_{700}) \quad (5)$$

or

$$\mathrm{FEY}(H_2) \approx (1.23\ \mathrm{eV} + 0.06\ \mathrm{eV}\ \mathrm{pH}_{H_2} - 0.06\ \mathrm{eV}\ \mathrm{pH}_{O_2})/3.60\ \mathrm{eV} \quad (6)$$

where pH_{O_2} and pH_{H_2} denote the pH at the place (or cellular compartment) of water oxidation and proton reduction, respectively. The pH dependence is formally given, but it is of minor interest with respect to the "harvestable" dihydrogen. Neglecting the pH difference, we arrive at a FEY value of 34%. This figure represents a maximal value assuming that all electrons removed from water are used for hydrogen reduction.

Taking into account also the efficiency of conversion of the incident solar radiation into excited states of P680 and E_{700} ($\eta_{Ant} = 34\%$) and a quantum yield of 90%, we arrive at a theoretical maximum of 10.5% for the total solar-energy conversion efficiency of H_2 production in photosynthetic cells (directly driven by PSII *and* PSI).

The above η_{Solar} of 10.5% for hydrogen production by photosynthetic cells represents a hypothetical maximum, not taking into account the essential energy requirement for the metabolism of the cell. A realistic target figure for photosyn-

thetic cells genetically optimized for hydrogen production ("H_2-design cell") may be 5%. For comparison, the maximal η_{Solar} for dry-matter production by higher plants is close to 5%, but only in exceptional cases the "real" dry-matter yield will exceed 1 or 2%.[6]

Quantum Yield (QY) and Overall Efficiency (η_{SOLAR})

The QY in eq 1 denotes the probability that P680* formation results in product formation along the main path of redox chemistry. It is determined by the competition between forward reactions and recombination processes.[17,23−25] Formation of $P680^+Q_A^-$ competes with the radiative (fluorescence) and nonradiative (thermal dissipation) decay of excited singlet states of antenna chlorophylls, as described by the RRP model;[14,15] the QY of $P680^+Q_A^-$ formation may be close to 95%.[14]

The QY of subsequent steps relates directly to the miss parameter (*M*) of the S-state model (QY = 1 − *M*).[20,23] This QY can be as high as 92% and is determined by loss processes which occur after $P680^+Q_A^-$ formation and result from the competition between charge recombination and forward reactions in the microsecond to millisecond time domain. At pH below 5, the QY is significantly lowered (M > 20%), at least for the oxygen-evolution transition ($S_3 \rightarrow S_0 + O_2$).[23,26,27]

In PSII, losses by direct charge recombination, by ET from Q_A^- to $P680^+$, are negligible. Decay after repopulation of excited singlet states of Chl is of less importance than back-reactions which result in the formation of the triplet state of $P680^+Phe^-$ (triplet probability of 75%). The $P680^+Phe^-$ triplet, however, is assumed to decay especially rapidly by recombination (∼300 ps), rendering $P680^+Phe^-$ formation by backward electron transfer the major loss process within microseconds to milliseconds after photon absorption.[17,23−25]

We assume that QY is 0.95 for the $P680^+Q_A^-$ radical formed within less than 1 ns and 0.875 (= 0.95 × 0.92) for products formed later. By combination of the numbers obtained for LHY, FEY, and QY (eq 1), the overall efficiency of solar energy conversion by PSII (η_{SOLAR}) is obtained for various reaction products (Figure 3).

Redox Potentials

Redox titrations of donor-side cofactors cannot be done without oxidative damage to cofactors and protein matrix. Moreover, due to electrostatic interactions, the relevant "working potential" for electron transfer from or to a specific PSII redox factor depends on the redox state of other cofactors as well as on the protonation-state pattern and transmembrane voltages.[17,28,29] Thus, the relevant E_m could differ significantly from a potential obtained by redox titrations using external reductants.[17] Only for the Q_A/Q_A^- couple a reasonable E_m has been determined by redox titrations, that is, −0.08 V for PSII membrane particles with a functional donor side and uninhibited Q_B site.[30] Using this E_m value as an anchor point, the working potentials of other PSII cofactors (Figure 5) can be derived from the free-energy differences of Figure 3 assuming

$$|E_{m1} - E_{m2}| \approx |\Delta G_{12}| \quad (7)$$

where ΔG_{12} is the free-energy difference determined experimentally for the ET between two redox factors (with E_{m1} and E_{m2}).[9,16,17,24,28,31]

(We note that the here relevant figures for ΔG_{12}, E_{m1}, and E_{m2} relate to the individual ET step so that ΔG_{12} corresponds to the ΔG_0 in ET theory. Consequently, ΔG_{12}, E_{m1}, and E_{m2} are largely independent of the concentration of reduced and oxidized species in an ensemble of PSII. For the actual ET step itself, the corresponding E_m-values are also pH-independent, at least to a first approximation. However, preceding or subsequent protonation reactions can change this working E_m.[17,29])

Overpotential and Energetics of PSII Water Oxidation

The energy loss is clearly lower at the PSII donor side than at the acceptor side (see Figure 5). This relates to the low "overpotential" of PSII water oxidation. In electrochemical water oxidation, the overpotential (η) is the difference between the H_2O/O_2 equilibrium potential and the anodic potential, V^+ (at room temperature, $\eta \approx V^+ - (1.23 - 0.06\ pH) \cdot V$). This value of η is adjustable by the experimentator because it depends on the selection of V^+ and pH. Somewhat confusingly, not only this adjustable η is called overpotential but also the specific minimal value (η_{min}) required for a distinct rate of water oxidation measured in terms of the associated anodic current (e.g., η_{min} is the η-value for a current of 1 mA per cm^2 of electrode area). The η_{min}-value (e.g., 0.5 V for a Pt electrode in 1 N KOH) is not an experimental variable but a performance parameter characterizing the energetic efficiency of the respective system.

The initial oxidant in water oxidation at the Mn complex of PSII is the Y_Z^+ as it is formed within nanoseconds after flash excitation. Its redox potential of 1.2 eV corresponds to the anodic potential in electrochemical water oxidation. The lowest pH for efficient water oxidation by PSII is around 5.5,[23,26,27] corresponding to an equilibrium potential of the H_2O/O_2 couple of about 0.9 V (at O_2 partial pressure of 1 bar). Thus, in PSII water oxidation, the performance-parameter

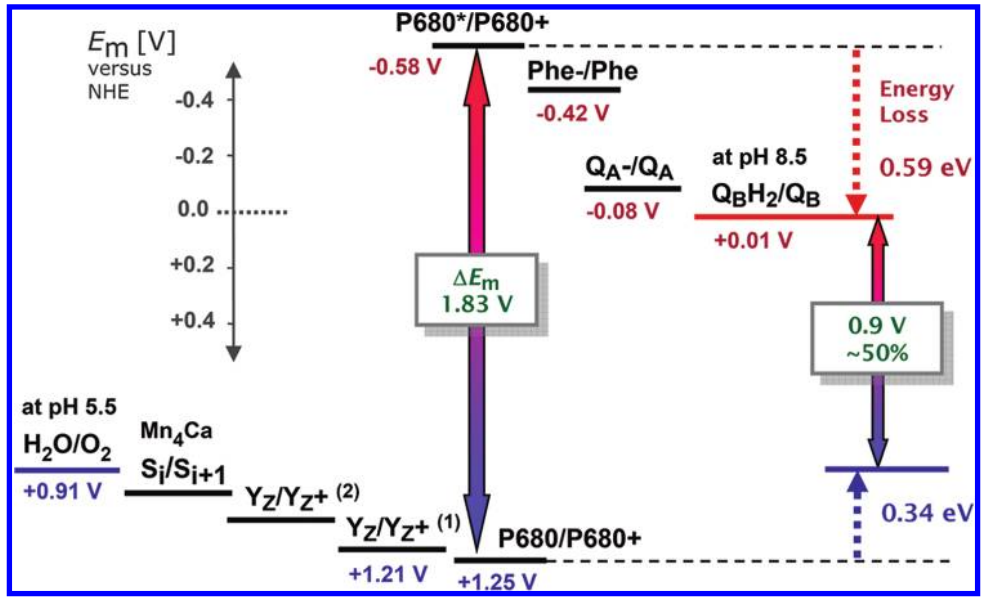

FIGURE 5. Estimated redox potentials (versus NHE).

"overpotential" is around 0.3 V. The corresponding energetic efficiency of 75% (= 0.9 V/1.2 V) is high, especially when taking into account that the water oxidation in PSII also is so fast (~2 ms) that it efficiently outcompetes recombination losses.

The overpotential represents the free-energy surplus of the process and resembles the driving force. For oxidation of two water molecules and O_2 release, the Y_Z^+ state of PSII is formed four times, resulting in a total ΔG surplus of 1.2 eV (at pH 5.5). This figure relates to the complete sequence of events in the water oxidation cycle involving steps of electron transfer, proton release, bond breaking and making, and dioxygen release. The current state of knowledge (and hypotheses) on *distribution* of the total free-energy surplus on various steps is summarized in Figure 6.

The scheme of Figure 6 roots in a basic model of the sequence electron transfer and proton release steps which has been described elsewhere.[29,32] The free-energy loss associated with the ET from the Mn complex to Y_Z^+ is given by the E_m difference between the Mn complex and Y_Z^+ (ΔE_{Mn-Z}) at the time of the electron transfer (eq 7). This ET and the associated ΔE_{Mn-Z} could include local rearrangements of hydrogen bonds and thus concerted, proton-coupled ET. However, this ET step (and thus $\Delta E_{Mn\text{-}Z}$) is not directly coupled to the process of removing a proton from the Mn complex and transferring it to the aqueous bulk phase.[18]

The free-energy difference associated with each of the four deprotonation steps (ΔG_i^{H+}, $i = 1-4$) is estimated according to

$$|\Delta G_i^{H+}| = 0.06\ \text{V}\ (\text{pH} - \text{p}K_i) \qquad (8)$$

where pK_i refers to the pK-value of the deprotonating group. Relatively high pK_i values minimize the free-energy loss (minimal $|\Delta G^{H+}|$) but limit the pH range for efficient water oxidation (inhibition for pH < pK_{Bi}). Results on the pH-dependent yield of individual S-state transitions suggest that the pK_{Bi} in the $S_3^+ \rightarrow S_3^n$ transition is close to 4.6 but lower in $S_2^+ \rightarrow S_2^n$ and $S_1^+ \rightarrow S_1^n$.[26] We note that each deprotonation in the scheme of Figure 6 is of direct relevance to the water oxidation chemistry: either a substrate water is directly deprotonated or a base at the Mn complex is created which can serve as a proton acceptor in the $S_4^+ \rightarrow S_0^+$ transition during which the O−O bond formation chemistry takes place.[18]

The release of dioxgen from its formation site and its dilution in the aqueous bulk is entropically driven and renders the total process of water oxidation energetically more favorable by ~0.27 eV, at an oxygen partial pressure (p_{O_2}) of 1 bar (0.31 eV at an atmospheric p_{O_2} of 0.21 bar).[18] One-fourth of this number is included in the standard one-electron potential of each of the four one-electron steps of water oxidation. However when dissecting the reaction into a sequence of steps, the entropic O_2 release matters only in the $S_3 \rightarrow S_0$ transition: After its formation, the O_2 molecule still is bound ($S_0^+ \cdots O_2$ in Figure 6); the entropic ΔG contribution from O_2 release likely overrides the (enthalpic) binding energy, as schematically shown in Figure 6.

If the free-energy gain of 0.27 V assignable to O_2 release were fully used to support the O_2-formation chemistry, inhibition of O_2 formation would be observable already at moderately increased p_{O_2}. The "thermodynamic" inhibition of O_2 formation at elevated p_{O_2} has been addressed experimentally only recently.[33−36] Initial findings appeared to support a low value of the half-inhibition p_{O_2} (2−3 bar).[33] However, by mon-

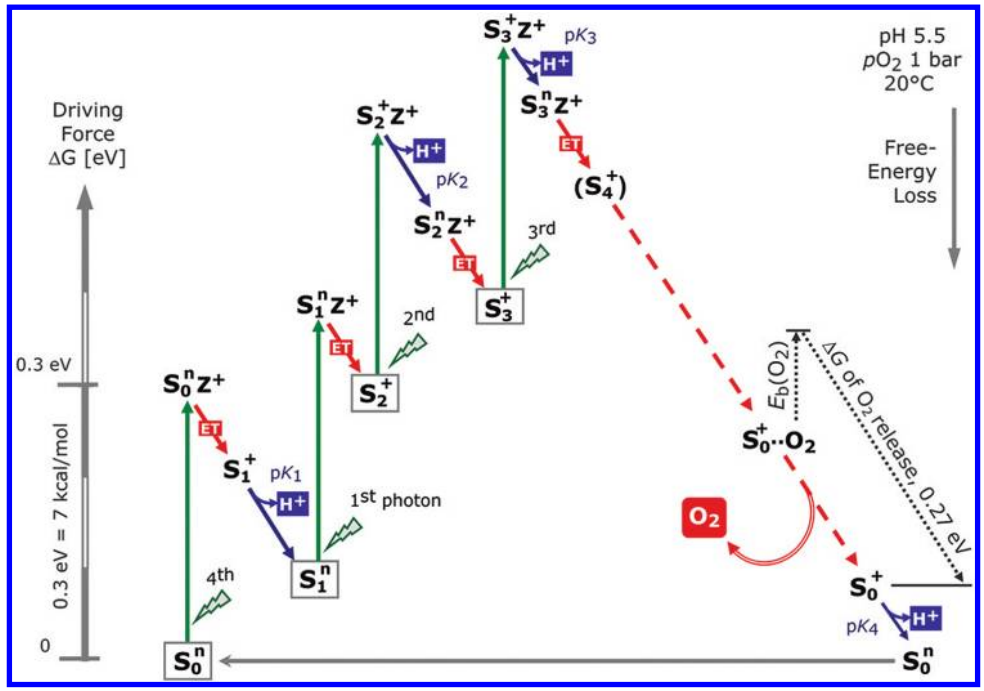

FIGURE 6. Energetic scheme of water oxidation at the PSII donor side. Green arrows, ΔG gain per photon; red arrows, ΔG loss of ET step from Mn complex to Y_Z; blue arrows, ΔG loss of deprotonation and proton release; red arrows/broken lines, ΔG loss of O_2 formation chemistry and O_2 release. The magnitudes of the free-energy changes (ΔG) represent rough estimates only; the value of the O_2 binding energy, $E_b(O_2)$, is unknown. The basic sequence of events is supported by experimental findings, but often evidence is still circumstantial and unsatisfactory, especially for all steps from $S_3{}^nZ^+$ to $S_0{}^n$.

itoring the Mn oxidation-state changes specifically by time-resolved X-ray measurements, no inhibition of the O_2-formation step was observed up to 16 bar and it has been concluded that any intermediate formed in the $S_3 \rightarrow S_0$ transition is by more than 130 meV higher in free energy than the final product state (i.e., $S_0 + O_2$).[35] Thus, a major fraction of the free-energy gain resulting from O_2 formation is not exploited for driving water oxidation. What appears to be a free-energy waste renders the O_2-formation step fully insensitive to increased dioxygen levels as encountered, for example, in microbial mats and alga cultures.

Binding of (substrate) water molecules to the Mn complex contributes to the energetics of water oxidation (however, the corresponding downward pointing arrow is not shown in Figure 6). Water binding closely associated with unbinding of dioxygen is plausible; then the arrow labeled as $E_b(O_2)$ would represent the difference between O_2 and H_2O binding energies.

We emphasize that presently the values of most energetic parameters are insufficiently precise (redox potentials, pK_i; ΔH of O_2 formation[37]) or fully unknown (O_2 and H_2O binding energies). Their precise experimental determination coupled to resolution of the underlying chemistry at the atomic level will be crucial for progress. Quantum chemical calculations[38] along the line of the energetic scheme of Figure 6 may facilitate numerical determination of energetic parameters that can be compared to experimentally accessible quantities, thereby providing the needed touchstones for evaluation of a calculated reaction path.

PSII in Its Native Environment: Light Saturation

In photovoltaic solar cells, an optimal match of photovoltage (U_{photo}) and photocurrent (I_{photo}) is required for maximal solar-energy conversion efficiency, as described by the filling factor. There is no corresponding quantity in photosynthesis. Yet the phenomenon of light saturation is related.

Light saturation of photosynthetic activity results in a decrease in the effective solar-energy conversion efficiency at increased light intensities. The numbers given above refer to an ideal situation where prior to the photon absorption event *all* PSIIs are ready to perform the light-driven reactions discussed above. For PSII in intact cells at high light intensities, however, the rate of CO_2 fixation limits the "electron flow" at the PSI acceptor side. This results in reduction of most components of the electron transfer chain and eventually in accumulation of PSII with a reduced primary quinone acceptor (Q_A^-). In the presence of Q_A^-, further light-driven ET to Q_A is impossible ("closed" PSII reaction center). In conclusion, high light intensities result in Q_A^- accumulation and consequently

reduction of the effective quantum yield detectable for an ensemble of PSII.[15,39]

The decrease in the effective yield of O_2 formation in response to an increased light intensity is more intricate than outlined above. It involves product backpressure (Q_A^- accumulation, increased lumenal proton concentration) as well as regulation and light-adaptation processes.[39,40] Moreover, photoinhibitory damage and the associated PSII repair cycle may lower the effective quantum yield of the total PSII complement present in a photosynthetic organism.[41]

Concluding Remarks

In PSII, the recombination lifetime of the $Z^+Q_A^-$-state is around 1 ms; the corresponding η_{SOLAR} exceeds 20%. These numbers suggest a performance level comparable to good silicon solar cells. However, a fair comparison is not that trivial. On the one hand, not all photosystems of an intact organism are working at optimal efficiency (light saturation, photoinhibition). On the other hand, in PSII, the energy is chemically stored and thus more valuable for direct fuel production than electrical energy. For example, the final PSII products are formed at an η_{SOLAR} of 16%, but this figure already includes the demanding water-oxidation process and thus is remarkably high. Clearly, the PSII can do its job at high efficiency and may serve as an inspiring model (and benchmark) for artificial systems.

A redesign of the light-driven PSII chemistry toward an improvement in the maximal value of η_{SOLAR} does not stand much of a chance. The energy loss reflected in the FEY-values in Figure 3 is largely essential for preventing quantum-yield reduction by back reactions. At the level of the final products (O_2/QH_2), around 0.9 eV of E_{680} is chemically stored whereas 0.9 eV is dissipated to ensure high quantum yield and quasi-irreversibility suggesting that, for the quinone acceptor used in nature, the E_{680}-value close to 1.8 eV is essentially without alternative.

Whereas the PSII chemistry is largely optimized, some improvement in η_{SOLAR} could result from use of additional antenna complexes which extend the absorption range to higher wavelengths, with unchanged E_{680}, as found in Chl *d*-containing cyanobacteria.[12,13] Mimicking synthetically the two-quantum process of H_2 formation driven by PSII and PSI, a clearly improved η_{SOLAR} could result from use of two "photosystems" with nonoverlapping absorption spectra and corresponding differences in the energy of the photochemistry-driving excited state (one "blue PS" and one "far-red PS").

With respect to the reduction of η_{SOLAR} by light saturation and photoinhibition, a reduction in the antenna size of PSII, for example, by eliminating the phycobilisome system in cyanobacteria, may be a fairly simple and efficient measure to improve the efficiency in a bioreactor at intermediate and high intensities of the incident sunlight. In a future photosynthetic organism genetically designed for biotechnological H_2 production, highly efficient use of electrons for proton reduction also may counteract light saturation by avoiding accumulation of reducing equivalents. The ATP requirement in cells reducing protons instead of CO_2 generally will be lowered so that a low thylakoid-PMF minimized by genetic engineering by partial "short-circuiting" (ion channels, "leaky" ATP synthase) could become "acceptable" to the cell and diminish the light saturation problem further.

Water oxidation at the Mn complex of PSII is a highly complex, multistep process, and we are only starting to understand kinetics and energetics of the individual steps at the atomic level. The scheme shown in Figure 6 may represent a useful conceptual framework for advanced quantitative considerations on the catalytic steps in photosynthetic water oxidation, a process that has shaped the biosphere and atmosphere and serves as an inspiration in the worldwide goal for solar-fuel technologies.

Financial support by the UniCat cluster of excellence (Unifying Concepts in Catalysis, Berlin), the German Ministry of Education and Research (BMBF, research consortia: Bio-H2 and H2 design cell), and the European Union (SOLAR-H2, #516510) is gratefully acknowledged.

BIOGRAPHICAL INFORMATION

Holger Dau received his doctoral degree in Kiel (in Physics, 1989), working with U.-P. Hansen on light adaptation of plants. After postdoctoral work with K. Sauer in Berkeley (1990−1992) and H. Senger in Marburg, he received his habilitation degree at the Biology Department of the Philipps University (Marburg, 1994). Since 2000, he has been a full professor in the Physics Department of the Free University in Berlin, where he investigates biological and synthetic metal sites with X-ray spectroscopy and complementary methods. His current focus lies on light-driven water oxidation and H_2 formation in biological and biomimetic systems.

Ivelina Zaharieva received her doctoral degree in 2003 in Sofia (Bulgaria), working with Vasilij Goltsev (Biophysics Department) on delayed light emission by plants. In 2007, she was awarded an Alexander-von-Humboldt fellowship for conducting research at the Free University Berlin, where she currently holds a position as a junior research scientist. She investigates PSII water oxidation by time-resolved fluorometric methods and employs X-ray spectroscopy to characterize transition metal sites in proteins and biomimetic complexes.

FOOTNOTES

*To whom correspondence should be addressed. Address: Freie Universität Berlin, FB Physik, Arnimallee 14, D-14195 Berlin, Germany. Telephone: +49-(0)30-838-53581. Fax: +49-(0)30-838-56299. E-mail: holger.dau@fu-berlin.de.

REFERENCES

1 Blankenship, R. E. *Molecular Mechanisms of Photosynthesis*; Blackwell Science: Oxford, England, 2002.

2 Ort, D.; Yocum, C. F. *Oxygenic Photosynthesis - The Light Reactions*; Kluwer Academic Publishers: Dordrecht, 1996; Vol. 10.

3 Bacon, K. *Photosynthesis - Photobiochemistry and Photobiophysics*; Kluwer Academic Publishers: Dordrecht, 2001.

4 Herrero, C.; Lassalle-Kaiser, B.; Leibl, W.; Rutherford, A. W.; Aukauloo, A. Artificial systems related to light driven electron transfer processes in PSII. *Coord. Chem. Rev.* **2008**, *252*, 456–468.

5 Magnuson, A.; Anderlund, M.; Johansson, O.; Lindblad, P.; Lomoth, R.; Polivka, T.; Ott, S.; Stensjö, K.; Styring, S.; Sundström, V.; Hammarström, L.,; Biomimetic and Microbial Approaches to Solar Fuel Generation. *Acc. Chem. Res.* **2009**, Doi: 10.1021/ar900127h.

6 Barber, J. Photosynthetic energy conversion: natural and artificial. *Chem. Soc. Rev.* **2009**, *38*, 185–196.

7 Ferreira, K. N.; Iverson, T. M.; Maghlaoui, K.; Barber, J.; Iwata, S. Architecture of the Photosynthetic Oxygen-Evolving Center. *Science* **2004**, *303*, 1831–1838.

8 Loll, B.; Kern, J.; Saenger, W.; Zouni, A.; Biesiadka, J. Towards complete cofactor arrangement in the 3.0 A resolution structure of photosystem II. *Nature* **2005**, *438*, 1040–1044.

9 Dau, H.; Sauer, K. Exciton equilibration and photosystem II exciton dynamics - a fluorescence study on photosystem II membrane particles of spinach. *Biochim. Biophys. Acta* **1996**, *1273*, 175–190.

10 Boichenko, V. A. Action spectra and functional antenna sizes of Photosystems I and II in relation to the thylakoid membrane organization and pigment composition. *Photosynth. Res.* **1998**, *58*, 163–174.

11 Schiller, H.; Huhn, M.; Dau, H. On the long-wavelength spectral forms of chlorophyll a in Photosystem I: Spectroscopic and immunological investigations on a greening mutant of the green alga Scenedesmus obliquus. *Photosynth. Res.* **1998**, *55*, 95–107.

12 Miyashita, H.; Ikemoto, H.; Kurano, N.; Adachi, K.; Chihara, M.; Miyachi, S. Chlorophyll d as a major pigment. *Nature* **1996**, *383*, 402.

13 Schiller, H.; Senger, H.; Miyashita, H.; Miyachi, S.; Dau, H. Light-harvesting in *Acaryochloris marina*—spectroscopic characterization of a chlorophyll d-dominated photosynthetic antenna system. *FEBS Lett.* **1997**, *410*, 433–436.

14 Schatz, G. H.; Brock, H.; Holzwarth, A. R. Kinetic and energetic model for the primary processes in photosystem II. *Biophys. J.* **1988**, *54*, 397–405.

15 Dau, H. Molecular mechanisms and quantitative models of variable photosystem II fluorescence. *Photochem. Photobiol.* **1994**, *60*, 1–23.

16 Grabolle, M.; Dau, H. Energetics of primary and secondary electron transfer in Photosystem II membrane particles of spinach revisited on basis of recombination-fluorescence measurements. *Biochim. Biophys. Acta* **2005**, *1708*, 209–218.

17 Rappaport, F.; Diner, B. A. Primary photochemistry and energetics leading to the oxidation of the $(Mn)_4Ca$ cluster and to the evolution of molecular oxygen in Photosystem II. *Coord. Chem. Rev.* **2008**, *252*, 259–272.

18 Dau, H.; Haumann, M. The manganese complex of photosystem II in its reaction cycle - Basic framework and possible realization at the atomic level. *Coord. Chem. Rev.* **2008**, *252*, 273–295.

19 Renger, G.; Renger, T. Photosystem II: The machinery of photosynthetic water splitting. *Photosynth. Res.* **2008**, *98*, 53–80.

20 Dau, H.; Haumann, M. Time-resolved X-ray spectroscopy leads to an extension of the classical S-state cycle model of photosynthetic oxygen evolution. *Photosynth. Res.* **2007**, *92*, 327–343.

21 Haumann, M.; Liebisch, P.; Muller, C.; Barra, M.; Grabolle, M.; Dau, H. Photosynthetic O_2 formation tracked by time-resolved X-ray experiments. *Science* **2005**, *310*, 1019–1021.

22 McEvoy, J. P.; Brudvig, G. W. Water-Splitting Chemistry of Photosystem II. *Chem. Rev.* **2006**, *106*, 4455–4483.

23 Grabolle, M.; Dau, H. Efficiency and role of loss processes in light-driven water oxidation by PSII. *Physiol. Plant.* **2007**, *131*, 50–63.

24 de Wijn, R.; van Gorkom, H. J. The rate of charge recombination in Photosystem II. *Biochim. Biophys. Acta* **2002**, *1553*, 302–308.

25 Cser, K.; Vass, I. Radiative and non-radiative charge recombination pathways in Photosystem II studied by thermoluminescence and chlorophyll fluorescence in the cyanobacterium Synechocystis 6803. *Biochim. Biophys. Acta* **2007**, *1767*, 233–243.

26 Bernat, G.; Morvaridi, F.; Feyziyev, Y.; Styring, S. pH-Dependence of the Four Individual Transitions in the Catalytic S-Cycle during Photosynthetic Oxygen Evolution. *Biochemistry* **2002**, *41*, 5830–5843.

27 Messinger, J.; Renger, G. Analyses of pH-Induced Modifications of the Period Four Oscillation of Flash-Induced Oxygen Evolution Reveal Distinct Structural Changes of the Photosystem II Donor Side at Characteristic pH Values. *Biochemistry* **1994**, *33*, 10896–10905.

28 Dau, H.; Sauer, K. Electric field effect on the picosecond fluorescence of photosystem II and its relation to the energetics and kinetics of primary charge separation. *Biochim. Biophys. Acta* **1992**, *1102*, 91–106.

29 Dau, H.; Haumann, M. Eight steps preceding O-O bond formation in oxygenic photosynthesis--a basic reaction cycle of the Photosystem II manganese complex. *Biochim. Biophys. Acta* **2007**, *1767*, 472–483.

30 Krieger, A.; Rutherford, A. W.; Johnson, G. N. On the determination of redox midpoint potential of the primary quinone electron acceptor, Q_A, in photosystem II. *Biochim. Biophys. Acta* **1995**, *1229*, 193–201.

31 Rappaport, F.; Guergova-Kuras, M.; Nixon, P. J.; Diner, B. A.; Lavergne, J. Kinetics and Pathways of Charge Recombination in Photosystem II. *Biochemistry* **2002**, *41*, 8518–8527.

32 Dau, H.; Haumann, M. Reaction cycle of photosynthetic water oxidation in plants and cyanobacteria. *Science* **2006**, *312*, 1471–1472.

33 Clausen, J.; Junge, W. Detection of an intermediate of photosynthetic water oxidation. *Nature* **2004**, *430*, 480–483.

34 Clausen, J.; Junge, W.; Dau, H.; Haumann, M. Photosynthetic Water Oxidation at High O_2 Backpressure Monitored by Delayed Chlorophyll Fluorescence. *Biochemistry* **2005**, *44*, 12775–12779.

35 Haumann, M.; Grundmeier, A.; Zaharieva, I.; Dau, H. Photosynthetic water oxidation at elevated dioxygen partial pressure monitored by time-resolved X-ray absorption measurements. *Proc. Natl. Acad. Sci. U.S.A.* **2008**, *105*, 17384–17389.

36 Kolling, D. R.; Brown, T. S.; Ananyev, G.; Dismukes, G. C. Photosynthetic Oxygen Evolution Is Not Reversed at High Oxygen Pressures: Mechanistic Consequences for the Water-Oxidizing Complex. *Biochemistry* **2009**, *48*, 1381–1389.

37 Krivanek, R.; Dau, H.; Haumann, M. Enthalpy changes during photosynthetic water oxidation tracked by time-resolved calorimetry using a photothermal beam deflection technique. *Biophys. J.* **2008**, *94*, 1890–1903.

38 Siegbahn, P. E. Theoretical Studies of O−O Bond Formation in Photosystem II. *Inorg. Chem.* **2008**, *47*, 1779–1786.

39 Dau, H. Short-term adaptation of plants to changing light intensities and its relation to photosystem II photochemistry and fluorescence emission. *J. Photochem. Photobiol., B* **1994**, *26*, 3–27.

40 Dau, H.; Hansen, U. P. Studies on the adaptation of intact leaves to changing light intensities by a kinetic analysis of chlorophyll fluorescence and oxygen evolution as measured by the photoacoustic signal. *Photosynth. Res.* **1989**, *20*, 59–83.

41 Aro, E. M.; Virgin, I.; Andersson, B. Photoinhibition of Photosystem II. Inactivation, protein damage and turnover. *Biochim. Biophys. Acta* **1993**, *1143*, 113–134.